Journal of Geophysical Research-Earth Surface

Supporting Information for

Exploring the Temporal-Varying and Depth-Nonlinear Velocity Profile of Debris Flows Based on A Stratification Statistical Algorithm for 3D-HBP-SPH Particles

Zheng HAN[1,2], Wendou XIE[1], Chuicheng ZENG[1], Yange LI[1,3*], Changli LI[1], Haohui DING[1], Weidong WANG[1], Ningsheng CHEN[4], Guisheng HU[4], Guangqi CHEN[5]

[1] School of Civil Engineering, Central South University, Changsha 410075, China.

[2] Hunan Provincial Key Laboratory for Disaster Prevention and Mitigation of Rail Transit Engineering Structures, Changsha 410075, China.

[3] The Key Laboratory of Engineering Structures of Heavy Haul Railway, Ministry of Education, Changsha 410075, China.

[4] Key Lab of Mountain Hazards and Surface Processes, Institute of Mountain Hazards and Environment, Chinese Academy of Sciences, Chengdu 610041, China.

[5] Department of Civil Engineering, Kyushu University, Fukuoka, 819-0395, Japan.

Corresponding author: Y. Li (liyange@csu.edu.cn), No.22 Shaoshan South Road, School of Civil Engineering, Central South University, Changsha, Hunan, China. Tel.: +86 18684982076.

Contents of this file

Text S1. The 3D-HBP-SPH numerical model of debris flow

To supplement the 3D-HBP-SPH numerical model of debris flow described in the main text, we briefly review the basics of this model here.

The 3D-HBP-SPH model refers to a numerical model used to describe the dynamic process of debris flow. The main feature of this model is that under the Lagrange form, the three-dimensional smooth particle hydrodynamics (3D-SPH) calculation framework is integrated with the Herschel-Bulkley-Papanastasiou (HBP) rheological model of debris flow. It is well known that in the 3D-SPH method, debris flow and other fluids are regarded as continuous incompressible fluids, characterized by a group of discrete particles, whose behavior can be described by solving the Navier-Stokes equation, which can provide a solution to obtain velocity fields in three dimensions. In addition, the HBP rheological model can more comprehensively reflect the possible nonlinear rheological characteristics of debris flow slurry under large deformation. Moreover, the HBP rheological model has better convergence than the Bingham model.

Therefore, the 3D-HBP-SPH model combining the above two advantages can effectively describe the dynamic process of debris flow under various complex conditions, our previous study (Han et al., 2019) has shown that the 3D-HBP-SPH model has good applicability in the analysis of the dynamic process of debris flow.

The HBP rheological model is expressed as follows:

$$\boldsymbol{\tau}^{\boldsymbol{\alpha\beta}} = 2\mu_{eff}\boldsymbol{\varepsilon}^{\boldsymbol{\alpha\beta}} \tag{1}$$

$$\boldsymbol{\varepsilon}^{\boldsymbol{\alpha\beta}} = \frac{\mathbf{1}}{\mathbf{2}}\left(\frac{\partial \boldsymbol{v}^{\boldsymbol{\alpha}}}{\partial \boldsymbol{x}^{\boldsymbol{\beta}}} + \frac{\partial \boldsymbol{v}^{\boldsymbol{\beta}}}{\partial \boldsymbol{x}^{\boldsymbol{\alpha}}}\right) \tag{2}$$

$$\mu_{eff} = 2^{n-1}\mu_B\dot{\gamma}^{n-1} + \frac{\tau_y}{2\dot{\gamma}}(1 - e^{-m\dot{\gamma}}) \tag{3}$$

$$\tau_y = coh + P\tan\varphi \tag{4}$$

Where, $\boldsymbol{\tau}^{\boldsymbol{\alpha\beta}}$ is the shear stress tensor, μ_{eff} is the equivalent viscosity coefficient, $\boldsymbol{\varepsilon}^{\boldsymbol{\alpha\beta}}$ is the local strain rate tensor, μ_B is the Bingham viscosity coefficient, m and n are the constant and power law index controlling the stress growth under different shear rates respectively, τ_y is the yield stress under the Mohr-Coulomb yield criterion, coh is the cohesive force of soil, φ is the Angle of internal friction, P represents normal stress, $\dot{\gamma}$ represents shear strain rate, which is defined as:

$$\dot{\gamma} = \frac{\sqrt{2}}{2}\boldsymbol{\varepsilon}^{\boldsymbol{\alpha\beta}} \tag{5}$$

In the Lagrange form, the Navier-Stokes equation composed of momentum conservation equation can be expressed as follows:

$$\frac{d\boldsymbol{v_i}^{\boldsymbol{\alpha}}}{dt} = -\sum_{j=1}^{N} m_j \left(\frac{P_i}{{\rho_i}^2} + \frac{P_j}{{\rho_j}^2}\right) \frac{\partial W_{ij}}{\partial {x_i}^{\alpha}}$$

$$+\sum_{j=1}^{N} m_j \left(\frac{2\mu_{effi}{\varepsilon_i}^{\alpha\beta}}{{\rho_i}^2} + \frac{2\mu_{effj}{\varepsilon_j}^{\alpha\beta}}{{\rho_j}^2}\right) \frac{\partial W_{ij}}{\partial {x_i}^{\beta}} + \boldsymbol{g}^{\boldsymbol{\alpha}} \tag{6}$$

Where, W_{ij} represents the kernel function; $\boldsymbol{v_i}^{\boldsymbol{\alpha}}$ and $\boldsymbol{g}^{\boldsymbol{\alpha}}$ represent particle velocity and gravity, respectively.

Please refer to our previous study (Han et al., 2019) for more details.

Figures S1 to S34. Summary of fitting results for 34 sets of experimental data

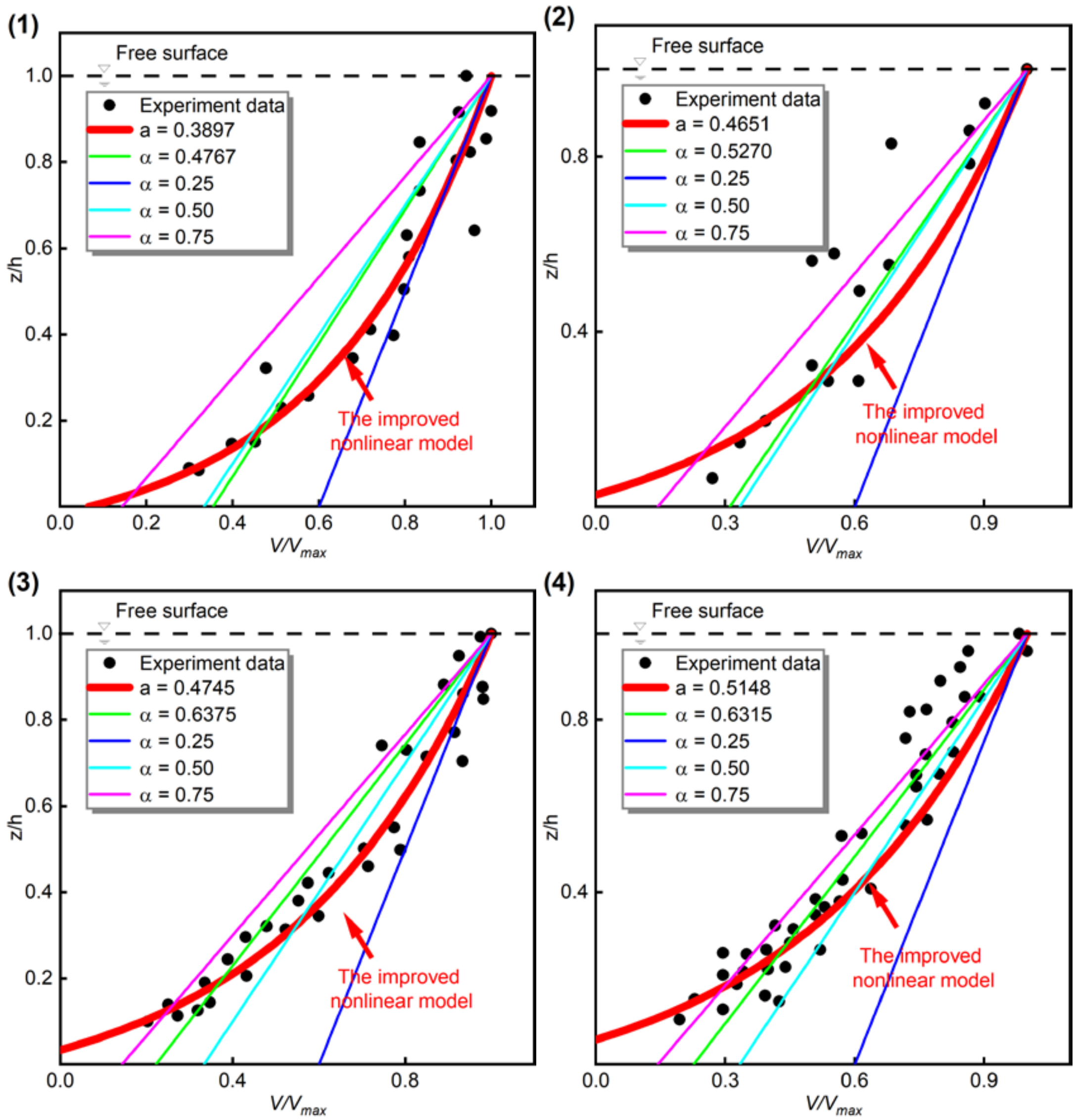

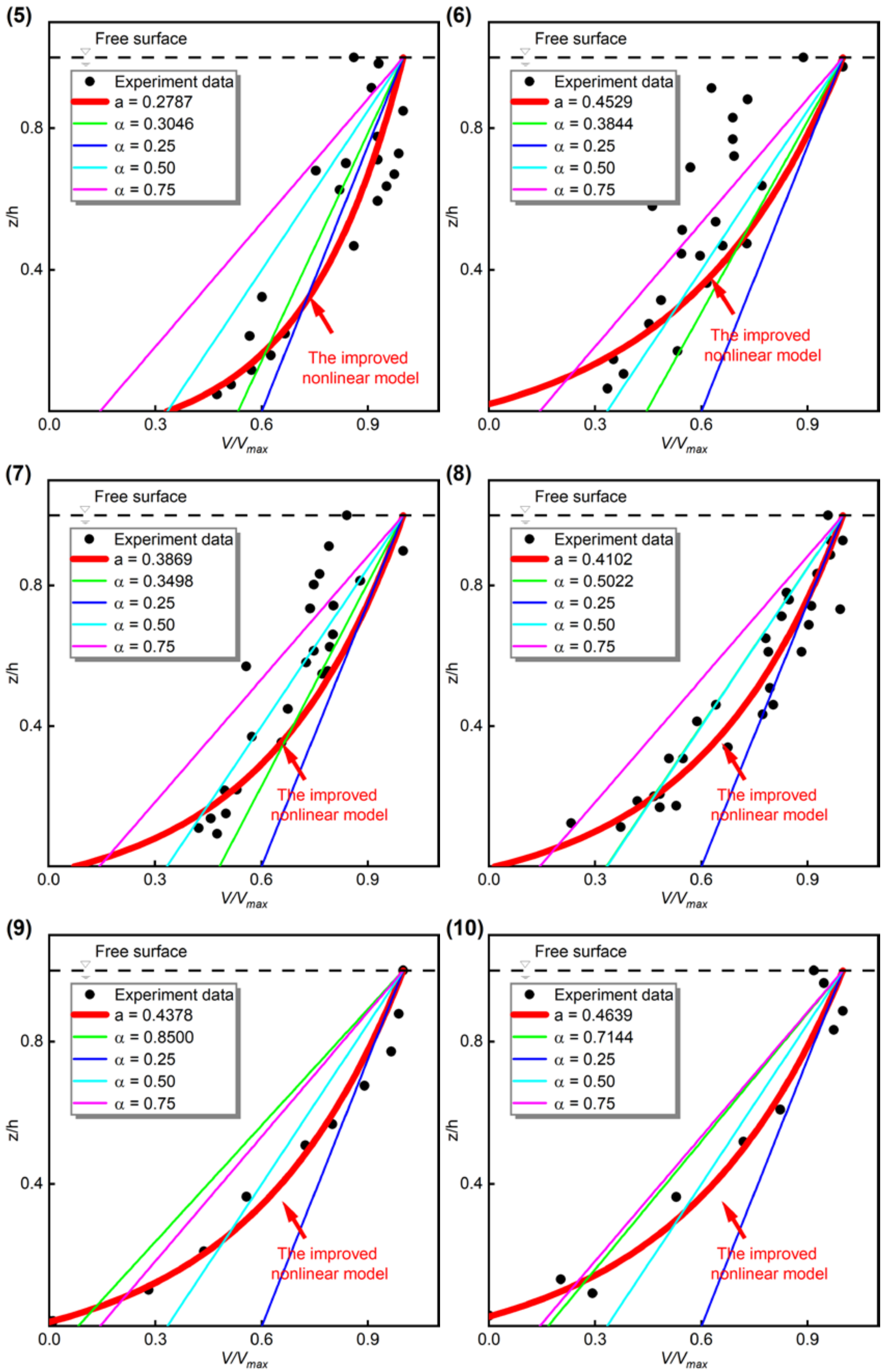
(5)
Free surface
Experiment data
a = 0.2787
α = 0.3046
α = 0.25
α = 0.50
α = 0.75
The improved nonlinear model
z/h
V/Vmax
0.0
0.3
0.6
0.9
0.4
0.8
(6)
Free surface
Experiment data
a = 0.4529
α = 0.3844
α = 0.25
α = 0.50
α = 0.75
The improved nonlinear model
z/h
V/Vmax
(7)
Free surface
Experiment data
a = 0.3869
α = 0.3498
α = 0.25
α = 0.50
α = 0.75
The improved nonlinear model
z/h
V/Vmax
(8)
Free surface
Experiment data
a = 0.4102
α = 0.5022
α = 0.25
α = 0.50
α = 0.75
The improved nonlinear model
z/h
V/Vmax
(9)
Free surface
Experiment data
a = 0.4378
α = 0.8500
α = 0.25
α = 0.50
α = 0.75
The improved nonlinear model
z/h
V/Vmax
(10)
Free surface
Experiment data
a = 0.4639
α = 0.7144
α = 0.25
α = 0.50
α = 0.75
The improved nonlinear model
z/h
V/Vmax

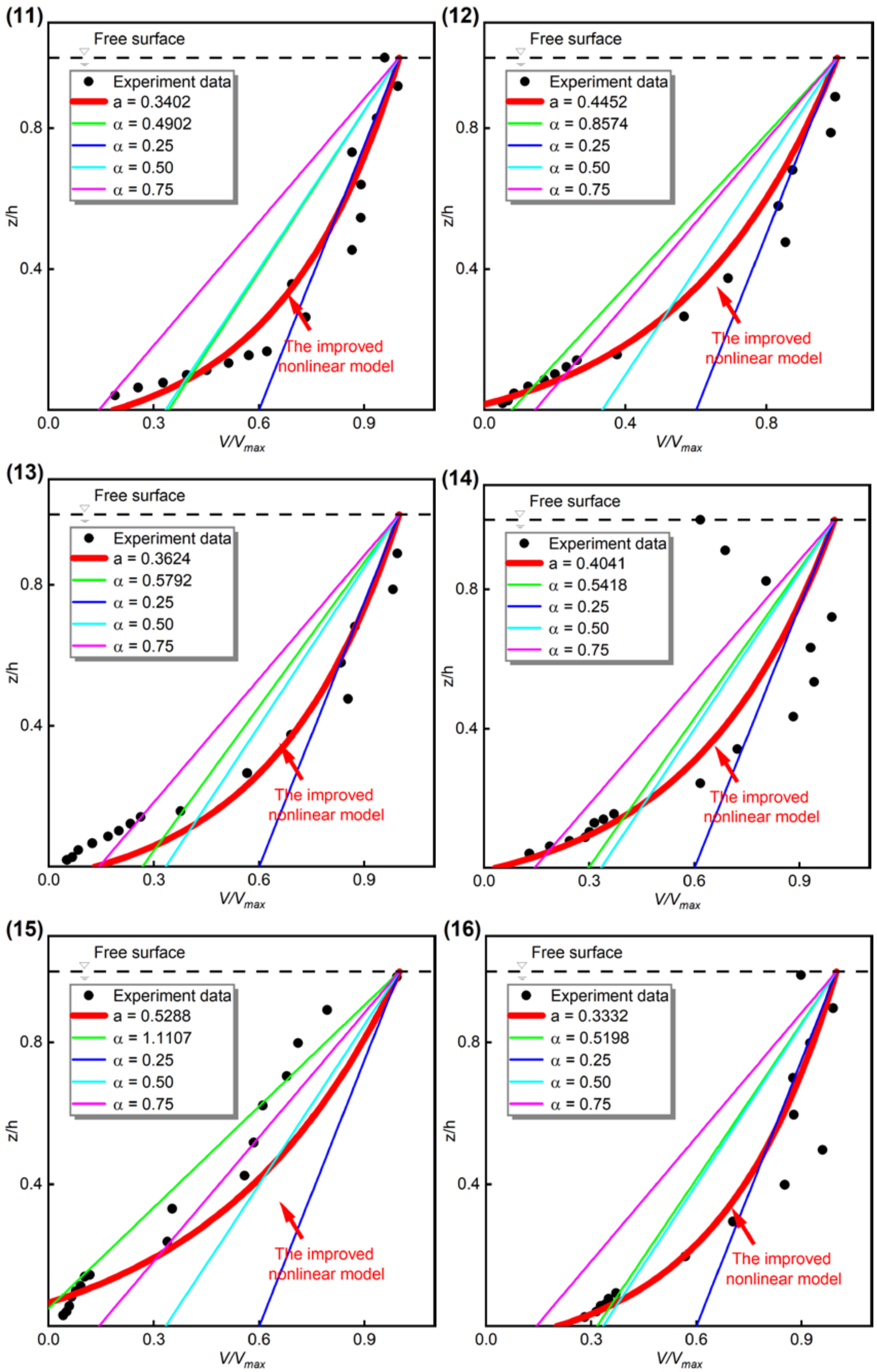
(11)
Free surface
Experiment data
a = 0.3402
α = 0.4902
α = 0.25
α = 0.50
α = 0.75
The improved nonlinear model
z/h
V/V_max
(12)
Free surface
Experiment data
a = 0.4452
α = 0.8574
α = 0.25
α = 0.50
α = 0.75
The improved nonlinear model
z/h
V/V_max
(13)
Free surface
Experiment data
a = 0.3624
α = 0.5792
α = 0.25
α = 0.50
α = 0.75
The improved nonlinear model
z/h
V/V_max
(14)
Free surface
Experiment data
a = 0.4041
α = 0.5418
α = 0.25
α = 0.50
α = 0.75
The improved nonlinear model
z/h
V/V_max
(15)
Free surface
Experiment data
a = 0.5288
α = 1.1107
α = 0.25
α = 0.50
α = 0.75
The improved nonlinear model
z/h
V/V_max
(16)
Free surface
Experiment data
a = 0.3332
α = 0.5198
α = 0.25
α = 0.50
α = 0.75
The improved nonlinear model
z/h
V/V_max

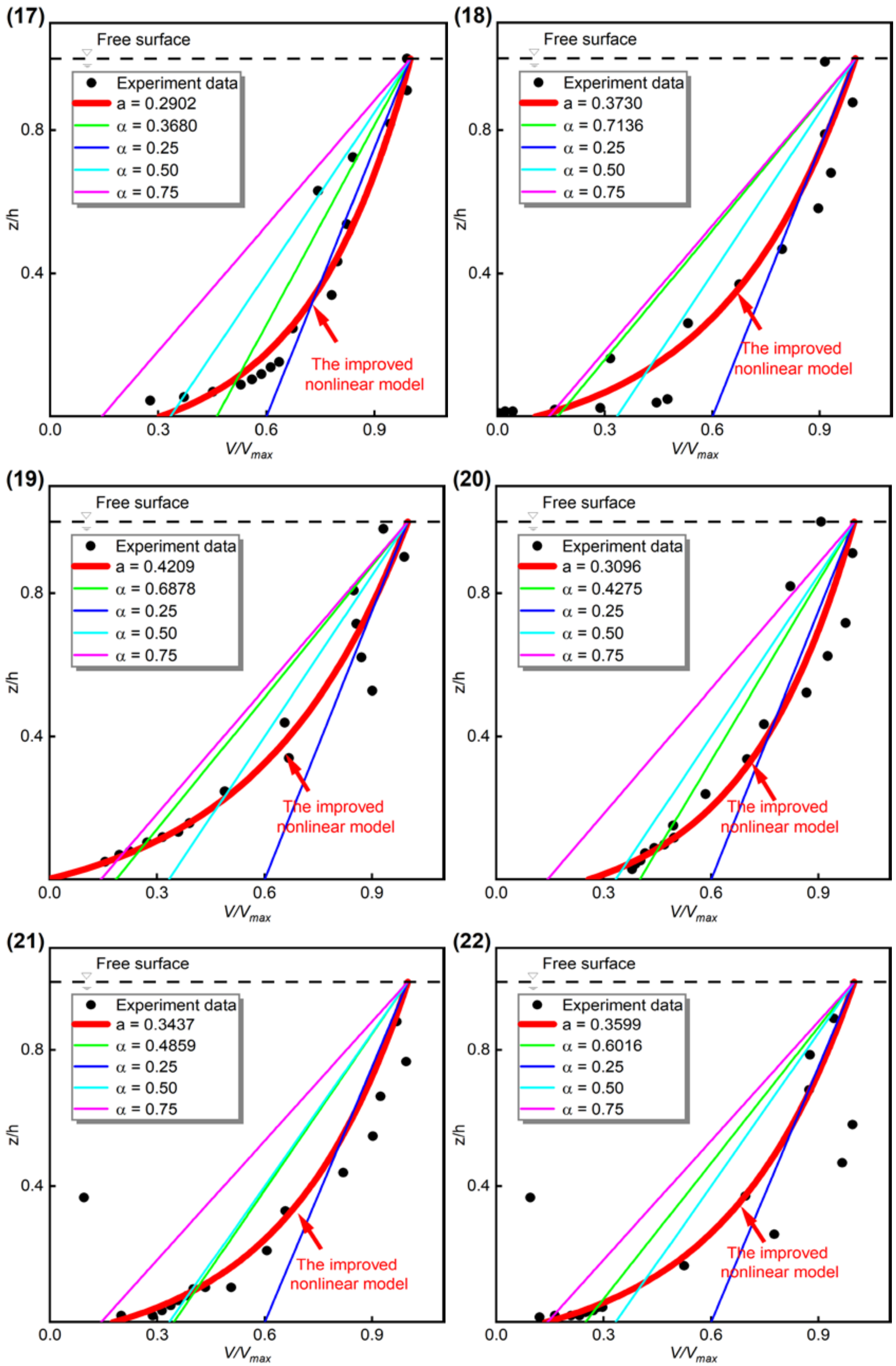
(17)
Free surface
Experiment data
a = 0.2902
α = 0.3680
α = 0.25
α = 0.50
α = 0.75
The improved nonlinear model
z/h
V/Vmax
(18)
Free surface
Experiment data
a = 0.3730
α = 0.7136
α = 0.25
α = 0.50
α = 0.75
The improved nonlinear model
z/h
V/Vmax
(19)
Free surface
Experiment data
a = 0.4209
α = 0.6878
α = 0.25
α = 0.50
α = 0.75
The improved nonlinear model
z/h
V/Vmax
(20)
Free surface
Experiment data
a = 0.3096
α = 0.4275
α = 0.25
α = 0.50
α = 0.75
The improved nonlinear model
z/h
V/Vmax
(21)
Free surface
Experiment data
a = 0.3437
α = 0.4859
α = 0.25
α = 0.50
α = 0.75
The improved nonlinear model
z/h
V/Vmax
(22)
Free surface
Experiment data
a = 0.3599
α = 0.6016
α = 0.25
α = 0.50
α = 0.75
The improved nonlinear model
z/h
V/Vmax

(23)

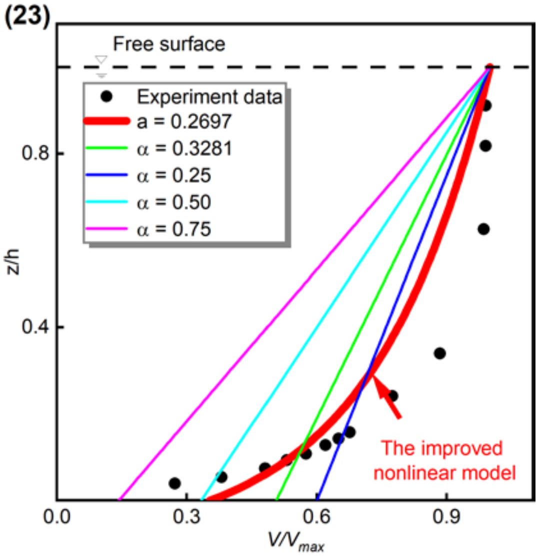

(24)

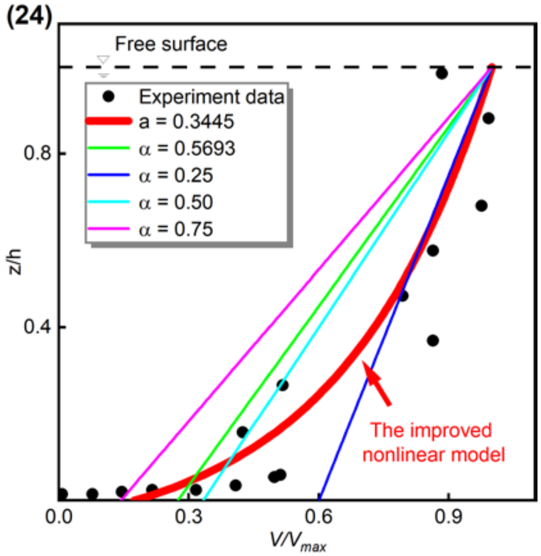

(25)

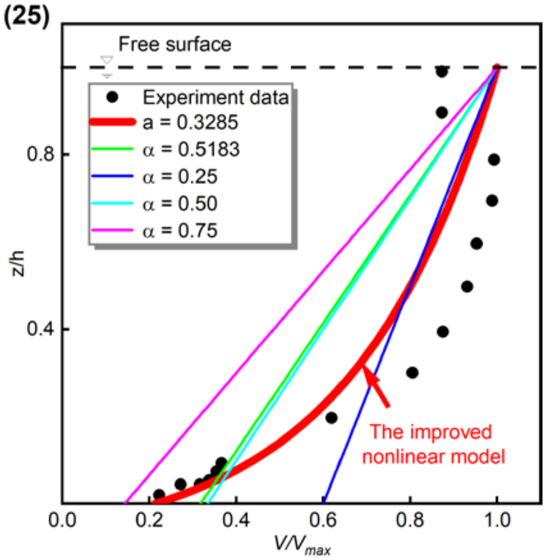

(26)

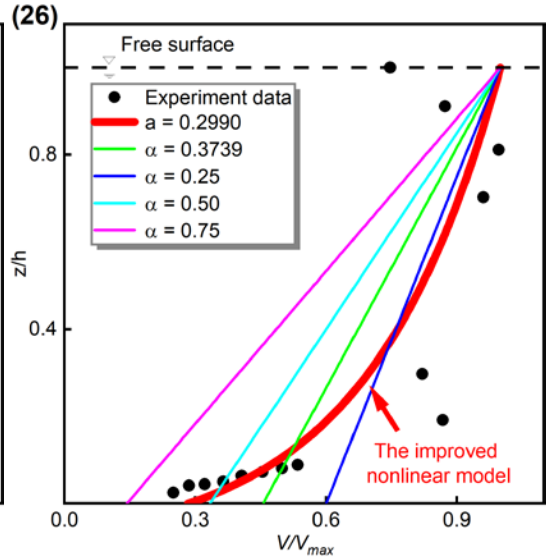

(27)

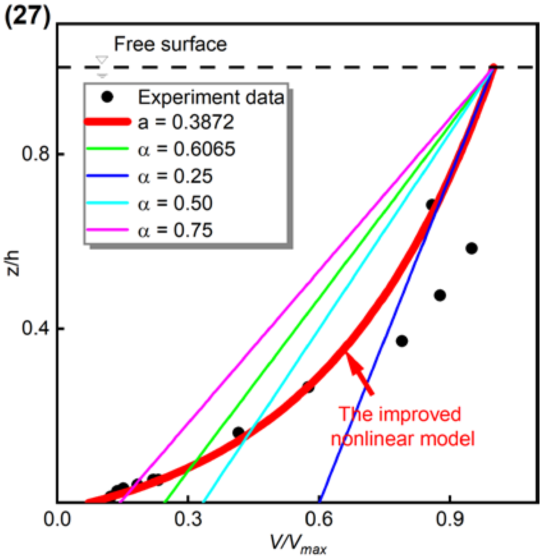

(28)

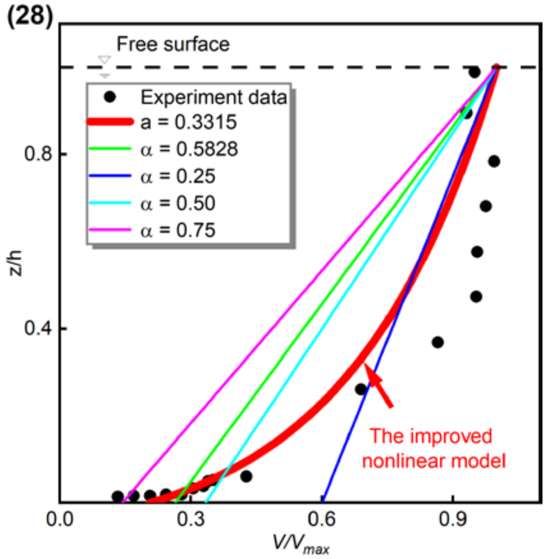

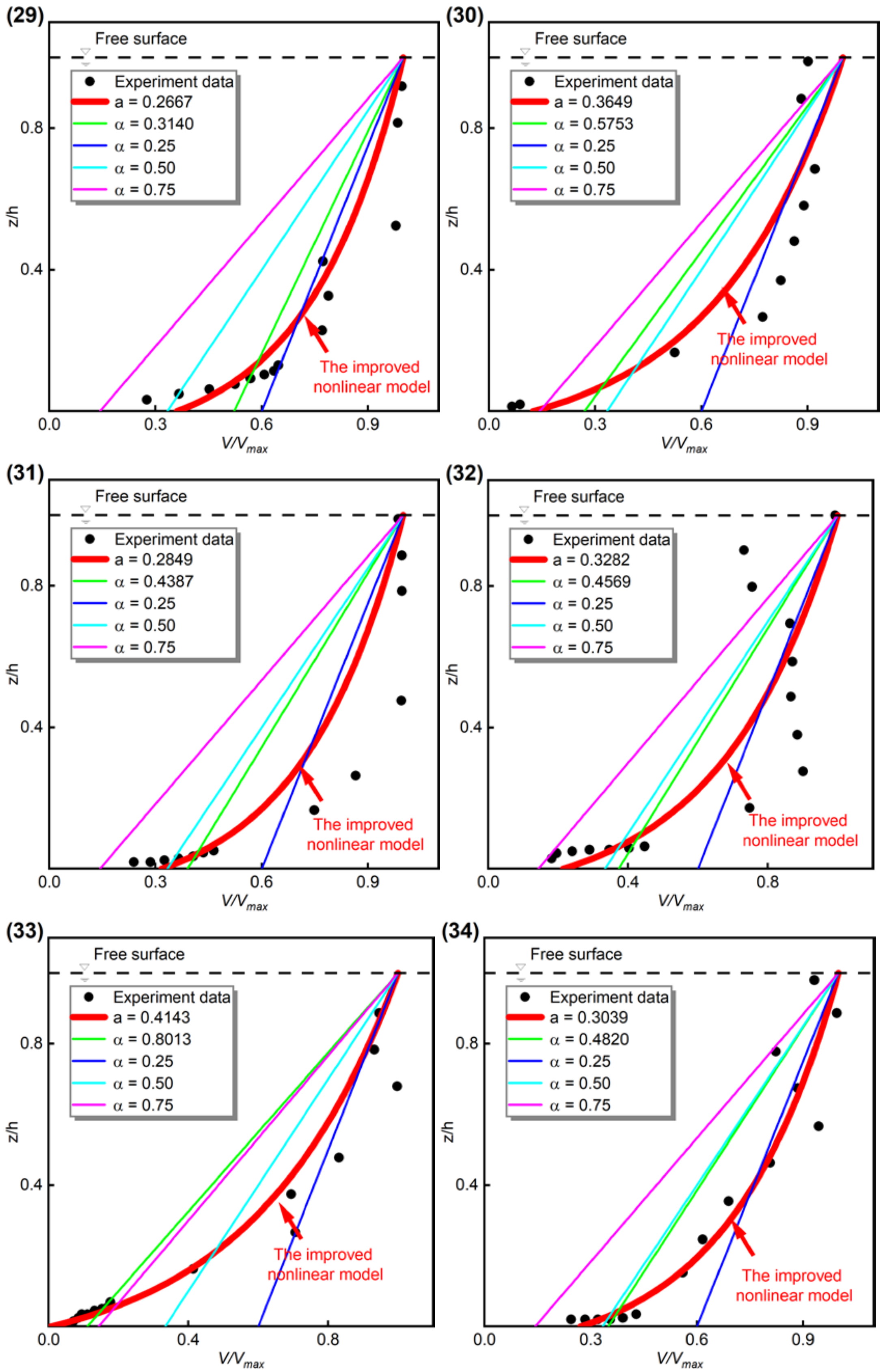

Figure S1 to S34. Summary of fitting results for 34 sets of experimental data.